Technische Universität Ilmenau
Institut für Mathematik

Nonlinear circuit models for the analysis of energetic systems

Büntig, Wolfgang G.; Vogt, Werner

September 1998

Nonlinear Circuit Models for the Analysis of Energetic Systems

W.G. Büntig, and W. Vogt
Technical University of Ilmenau
Dept. of Theoretical Basics of Electrical Engineering
and
Dept. of Mathematics
D-98684 Ilmenau GERMANY
wolfgang.buentig@e-technik.tu-ilmenau.de
vogt@mathematik.tu-ilmenau.de

1 Introduction

An energetic system is composed by a large number of subsystems. Modelling is difficult because of its complexity and the nonlinear behaviour of some system parts with hysteresis and saturated iron cores. A linear description is allowed only in restricted cases. The behaviour of the system is determined by a large number of parameters. So it is necessary for analysing the system to divide it in small particular systems, which can be described by simple nonlinear models with few parameters. Then one can analyse the properties of these systems by using the methods of dynamic analysis.

The first aim of our contribution is to demonstrate how it is possible to describe a simple energetic system with a nonlinear load and a linear generator. Especially we discuss the form of the differential equations and the effect of coupling between the equations. In some practical cases even harmonics in the voltage are observed. We can find already in our simple models that this is caused by distortions of the nonlinear load. Because of these even harmonics we can also observe a surmounting of voltage-amplitude of the dominant mode.

The second aim is to verify numerically the occurence of chaotic and quasi-periodic responses in these simple energetic systems. Beginning with unstable periodic responses and their Poincaré maps we approximate both stable and unstable invariant manifolds. With the help of a numerical continuation procedure we can detect transversal intersections of manifolds as an indicator of chaotic behaviour. Finally it will be demonstrated that quasi-periodic responses of the systems can be found. They are approximated by a geometrical- numerical method, which also includes the possibility of parameter continuation.
The description of an energetic system with the more realistic nonlinear model is a possible step in nonlinear modelling of such a system.

2 Model Equations

The **generator** may be linear and symmetric

$$e_R(t) = \hat{E}_0 \sin \omega t \qquad e_S(t) = \hat{E}_0 \sin(\omega t - 2\pi/3) \qquad e_T(t) = \hat{E}_0 \sin(\omega t - 4\pi/3). \tag{1}$$

Some general **normalization relations**

$$X_R = \omega L_R \quad X_S = \omega L_S \quad X_T = \omega L_T \qquad\qquad X_D = \omega L_D \quad X_E = \omega L_E \quad X_F = \omega L_F \tag{2}$$

$$X_{CR} = 1/\omega C_R \qquad X_{CS} = 1/\omega C_S \qquad X_{CT} = 1/\omega C_T \tag{3}$$

$$\tau = \omega t \quad U_0 = \omega \psi_0 \quad Z_0 = U_0/I_0 \qquad x = \psi/\psi_0 \quad y = i/I_0 \quad z = u/U_0 = u/(\omega \psi_0) \quad e_n = e/U_0 \tag{4}$$

The **nonlinear load** of a phase can be assumed by the circuit which is shown on Fig.1. An additional index R, S, and T is used to distiguish the three phases.

R_1 - Copper-resistance of the power supply and of the magnetic circuit

L_1 - Inductance of the power supply and leakage inductance of the magnetic circuit

C - Interturn capacitance and/or outer parallel capacitance

$i_L(\psi)$ - Characteristic function for describing the nonlinear iron core

R - Load resistance and/or resistance for modelling the hysteresis behaviour.
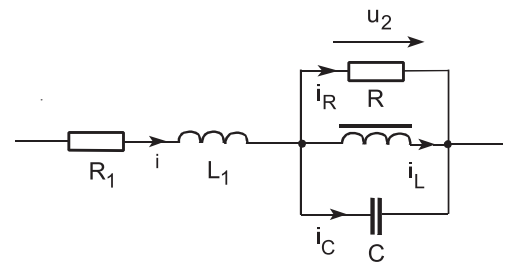

Fig. 1: General Load of one Phase

An incomplete power polynomial of the form $i_L(\psi) = a^* \psi + b^* \psi^n$ can be used to approximate the magnetization curve. The value of the exponent may be $n = 3$ or more realistic $n = 9$. A simple typical model of an energetic system is shown on Fig. 3. The system has a star-star structure. To analyse the properties of this

system we may observe some special cases with or without mid conductor; with a common magnetic core or with different magnetic systems. If the magnetic system has a common magnetic core the condition

$$\psi_R + \psi_S + \psi_T = 0 \tag{5}$$

has to be fullfiled. This condition leads to

$$\frac{d\psi_R}{dt} + \frac{d\psi_S}{dt} + \frac{d\psi_R}{dt} = 0 \rightsquigarrow u_R + u_s + u_T = 0 \tag{6}$$

It reduces the number of necessary differential equations.

2.1 Hysteresis Behaviour of the Load

The parallel connection of the linear resistance R and the non-linear inductor describes a hysteresis loop. For the approximation of the magnetization curve we use after Professor Philippow (see [1]) $i_L(\psi) = a^* \, \psi + b^* \, \psi^9$. If we assume an sinusoidal flux $\psi = \hat{\Psi} \sin \omega t$ then with $u_2 = \frac{d\psi}{dt} = \omega \hat{\Psi} \sqrt{1 - \left(\frac{\psi}{\hat{\Psi}}\right)^2}$ and $i_R = u_2/R$ we find $i_R(\psi)$. Then $i_H(\psi) = i_L(\psi) \pm i_R(\psi)$ in the normalized form

Fig. 2: Hysteresis loops for k=0.2 and k=0.4

$$y(x) = a \, x + b \, x^9 \pm k \sqrt{1 - x^2} = 0.25 \, x + 0.75 \, x^9 \pm k \sqrt{1 - x^2} \tag{7}$$

2.2 General Model with non-ideal Neutral Conductor

The energetic system is being described by the set of the state variables $i_R, i_S, i_T, u_R, u_S, u_T, \psi_R, \psi_S$, and ψ_T. In the normalized equations are being used some short cuts and prescriptions.

$$
\begin{aligned}
\Delta &= L_{1R}L_{1S}L_{1T} + L_0\left(L_{1R}L_{1S} + L_{1R}L_{1T} + L_{1S}L_{1T}\right) \\
L_R &= \Delta/[L_{1S}L_{1T} + L_0\left(L_{1S} + L_{1T}\right)] \qquad L_S = \Delta/[L_{1R}L_{1T} + L_0\left(L_{1R} + L_{1T}\right)] \\
L_T &= \Delta/[L_{1R}L_{1S} + L_0\left(L_{1R} + L_{1S}\right)] \\
L_D &= \Delta/[L_{1R}L_0] \qquad L_E = \Delta/[L_{1S}L_0] \qquad L_F = \Delta/[L_{1T}L_0]
\end{aligned}
\tag{8}
$$

We find in the general case with neutral conductor and different magnetic systems the following differential equations for the normalized Flux x, current y, and voltage z.

$$\frac{dx_R}{d\tau} = z_R \qquad \frac{dx_S}{d\tau} = z_S \qquad \frac{dx_T}{d\tau} = z_T \tag{9}$$

$$
\begin{aligned}
\frac{dy_R}{d\tau} &= \frac{Z_0}{X_R}e_{Rn} - \frac{Z_0}{X_F}e_{Sn} - \frac{Z_0}{X_E}e_{Tn} + \left[-\frac{R_{1R} + R_0}{X_R} + \frac{R_0}{X_F} + \frac{R_0}{X_E}\right]y_R \\
&+ \left[-\frac{R_0}{X_R} + \frac{R_{1S} + R_0}{X_F} + \frac{R_0}{X_E}\right]y_S + \left[-\frac{R_0}{X_R} + \frac{R_0}{X_F} + \frac{R_{1T} + R_0}{X_E}\right]y_T \\
&- \frac{Z_0}{X_R}z_R + \frac{Z_0}{X_F}z_S + \frac{Z_0}{X_E}z_T
\end{aligned}
\tag{10}
$$

$$
\begin{aligned}
\frac{dy_S}{d\tau} &= -\frac{Z_0}{X_F}e_{Rn} + \frac{Z_0}{X_S}e_{Sn} - \frac{Z_0}{X_D}e_{Tn} + \left[\frac{R_{1R} + R_0}{X_F} - \frac{R_0}{X_S} + \frac{R_0}{X_D}\right]y_R \\
&+ \left[\frac{R_0}{X_F} - \frac{R_{1S} + R_0}{X_S} + \frac{R_0}{X_D}\right]y_S + \left[\frac{R_0}{X_F} - \frac{R_0}{X_S} + \frac{R_{1T} + R_0}{X_D}\right]y_T \\
&+ \frac{Z_0}{X_F}z_R - \frac{Z_0}{X_S}z_S + \frac{Z_0}{X_D}z_T
\end{aligned}
\tag{11}
$$

$$\frac{dy_T}{d\tau} = -\frac{Z_0}{X_E}e_{Rn} - \frac{Z_0}{X_D}e_{Sn} + \frac{Z_0}{X_T}e_{Tn} + \left[\frac{R_{1R} + R_0}{X_E} + \frac{R_0}{X_D} - \frac{R_0}{X_T}\right]y_R$$

$$+ \left[\frac{R_0}{X_E} + \frac{R_{1S} + R_0}{X_D} - \frac{R_0}{X_T}\right]y_S + \left[\frac{R_0}{X_E} + \frac{R_0}{X_D} - \frac{R_{1T} + R_0}{X_T}\right]y_T \qquad (12)$$

$$+ \frac{Z_0}{X_E}z_R + \frac{Z_0}{X_D}z_S - \frac{Z_0}{X_T}z_T$$

$$\frac{dz_R}{d\tau} = \frac{X_{CR}}{Z_0}\left[y_R - \frac{Z_0}{R_R}z_R - a_R x_R - b_R x_R^n\right] \qquad \frac{dz_S}{d\tau} = \frac{X_{CS}}{Z_0}\left[y_S - \frac{Z_0}{R_S}z_S - a_S x_S - b_S x_S^n\right] \qquad (13)$$

$$\frac{dz_T}{d\tau} = \frac{X_{CT}}{Z_0}\left[y_T - \frac{Z_0}{R_T}z_T - a_T x_T - b_T x_T^n\right]$$
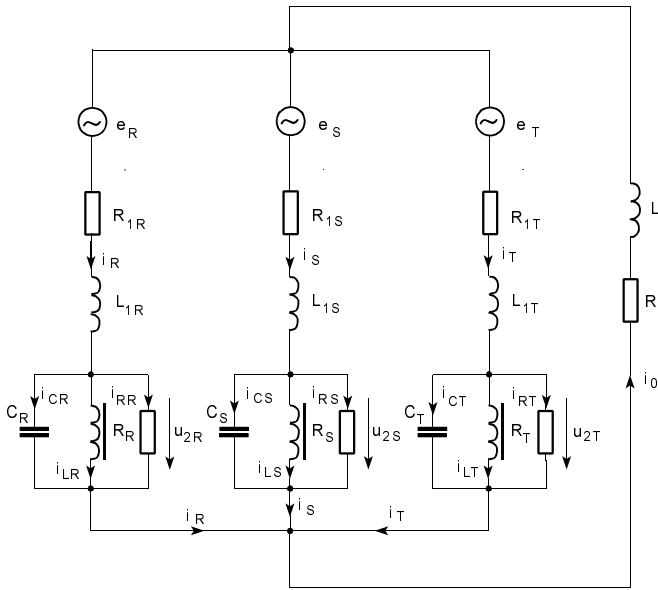

Fig. 3: Star-star form of a three-phase system

The simplest form of these equations will be reached if we assume an ideal neutral conductor $R_0 \approx 0$ and $L_0 \approx 0$. It leads to

$$L_R = L_{1R} \quad L_S = L_{1S} \quad L_T = L_{1T}$$
$$1/X_D = 0 \quad 1/X_E = 0 \quad 1/X_F = 0.$$

The system of the normalized differential equations (9) to (13) for the three phases are now not connected to each other. So we will find three independent differential equations of third order for the normalized flux. The solutions for this equation is discussed in detail in [2]. Some informations to parameter range

$$\omega L_{1R}/Z_0, \quad \omega L_{1S}/Z_0, \quad \omega L_{1T}/Z_0 \to 0,03...0,05$$
$$R_{1R}/Z_0, \quad R_{1S}/Z_0, \quad R_{1T}/Z_0 \to 0,03...0,05$$
$$\omega L_{1R}/R_R, \quad \omega L_{1S}/R_S, \quad \omega L_{1T}/R_T \to 0,0...0,5$$
$$X_{CR}/Z_0, \quad X_{CS}/Z_0, \quad X_{CT}/Z_0 \to 0,8...1,2$$

In the case of a common magnetic core you find for the normalized magnetization curve with $n = 9 \to a = 0,25$ and $b = 0,75$. This values may be used as basic for the variation of a and b in the case with different magnetic systems.

2.3 General Model without Neutral Conductor

If the model is without a neutral conductor $i_0 = 0 \quad \Rightarrow \quad i_T$ is dependent of i_R and i_S. In this case the equations for the normalized flux x and for the normalized voltage z are the same as in the case with neutral conductor. The equations for the normalized current y we have new to derive.
In the normalized equations are being used some short cuts and prescriptions.

$$\Delta = L_{1R}L_{1S} + L_{1R}L_{1T} + L_{1S}L_{1T}$$
$$L_R = \Delta/[L_{1S} + L_{1T}] \qquad L_S = \Delta/[L_{1R} + L_{1T}] \qquad (14)$$
$$L_D = \Delta/L_{1R} \qquad L_E = \Delta/L_{1S} \qquad L_F = \Delta/L_{1T}.$$

We find in the general case without neutral conductor and different magnetic systems the following differential equations for the normalized Flux x, current y, and voltage z.

$$\frac{dx_R}{d\tau} = z_R \qquad \frac{dx_S}{d\tau} = z_S \qquad \frac{dx_T}{d\tau} = z_T$$

$$\frac{dy_R}{d\tau} = \frac{Z_0}{X_R}e_{Rn} - \frac{Z_0}{X_F}e_{Sn} - \frac{Z_0}{X_E}e_{Tn} + \left[-\frac{R_{1R} + R_{1T}}{X_R} + \frac{R_{1T}}{X_F}\right]y_R$$
$$+ \left[-\frac{R_{1T}}{X_R} + \frac{R_{1S} + R_T}{X_F}\right]y_S - \frac{Z_0}{X_R}z_R + \frac{Z_0}{X_F}z_S + \frac{Z_0}{X_E}z_T \qquad (15)$$

$$\frac{dy_S}{d\tau} = -\frac{Z_0}{X_F}e_{Rn} + \frac{Z_0}{X_S}e_{Sn} - \frac{Z_0}{X_D}e_{Tn} + \left[\frac{R_{1R} + R_{1T}}{X_F} - \frac{R_{1T}}{X_S}\right]y_R$$
$$+ \left[\frac{R_{1T}}{X_F} - \frac{R_{1S} + R_{1T}}{X_S}\right]y_S + \frac{Z_0}{X_F}z_R - \frac{Z_0}{X_S}z_S + \frac{Z_0}{X_D}z_T \qquad (16)$$

$$\frac{dz_R}{d\tau} = \frac{X_{CR}}{Z_0}\left[y_R - \frac{Z_0}{R_R}z_R - a_R x_R - b_R x_R^n\right] \qquad \frac{dz_S}{d\tau} = \frac{X_{CS}}{Z_0}\left[y_S - \frac{Z_0}{R_S}z_S - a_S x_S - b_S x_S^n\right]$$
$$\frac{dz_T}{d\tau} = \frac{X_{CT}}{Z_0}\left[y_T - \frac{Z_0}{R_T}z_T - a_T x_T - b_T x_T^n\right]$$

If we assume a common iron core the equations will be reduced only to six because of the conditions eq.(5) and eq.(6).

$$\frac{dx_R}{d\tau} = z_R \qquad\qquad \frac{dx_S}{d\tau} = z_S$$

$$\frac{dy_R}{d\tau} = \frac{Z_0}{X_R}e_{Rn} - \frac{Z_0}{X_F}e_{Sn} - \frac{Z_0}{X_E}e_{Tn} + \left[-\frac{R_{1R} + R_{1T}}{X_R} + \frac{R_{1T}}{X_F}\right]y_R$$
$$+ \left[-\frac{R_{1T}}{X_R} + \frac{R_{1S} + R_T}{X_F}\right]y_S - \left[\frac{Z_0}{X_R} + \frac{Z_0}{X_E}\right]z_R + \left[\frac{Z_0}{X_F} - \frac{Z_0}{X_E}\right]z_S$$
$$\frac{dy_S}{d\tau} = -\frac{Z_0}{X_F}e_{Rn} + \frac{Z_0}{X_S}e_{Sn} - \frac{Z_0}{X_D}e_{Tn} + \left[\frac{R_{1R} + R_{1T}}{X_F} - \frac{R_{1T}}{X_S}\right]y_R$$
$$+ \left[\frac{R_{1T}}{X_F} - \frac{R_{1S} + R_{1T}}{X_S}\right]y_S + \left[\frac{Z_0}{X_F} - \frac{Z_0}{X_D}\right]z_R - \left[\frac{Z_0}{X_S} + \frac{Z_0}{X_D}\right]z_S$$

$$\frac{dz_R}{d\tau} = \frac{X_{CR}}{Z_0}\left[y_R - \frac{Z_0}{R_R}z_R - a_R x_R - b_R x_R^n\right] \qquad\qquad \frac{dz_S}{d\tau} = \frac{X_{CS}}{Z_0}\left[y_S - \frac{Z_0}{R_S}z_S - a_S x_S - b_S x_S^n\right]$$

The amplitudes of the forcing terms depend on the (varying) parameter λ via

$$\hat{\Gamma}_{R_1} = \frac{Z_0}{X_R}\frac{\hat{E}_0}{U_0} = 30.0\lambda, \quad \hat{\Gamma}_{R_2} = \frac{Z_0}{X_F}\frac{\hat{E}_0}{U_0} = 20.0\lambda, \quad \hat{\Gamma}_{R_3} = \frac{Z_0}{X_E}\frac{\hat{E}_0}{U_0} = 10.0\lambda .$$

2.4 Remarks to special Forms of Model-Equations

In all we can formulate six possible models - there are the following independent categories :

- with neutral conductor
  - ideal neutral conductor ($R_0 \approx 0; \quad L_0 \approx 0$)
  - non-ideal neutral conductor ($R_0 \neq 0; \quad L_0 \neq 0$)
- without neutral conductor ($R_0 \to \infty; \quad i_0 = 0$)
- one magnetic systems with a common iron core
- general magnetic model, non-common iron core.

3 Numerical Analysis

For $\lambda \in [1.0, 6.0]$, the following **types of solutions** could be observed:

- Beginning with $\lambda = 1.0$, a *stable solution* with period $T = 2\pi$ (see Figs. 4, 5) can be continuated numerically by a Newton-like method (TABHET) up to $\lambda = 3.0$ (see Figs. 6, 7), where stability is guaranteed.
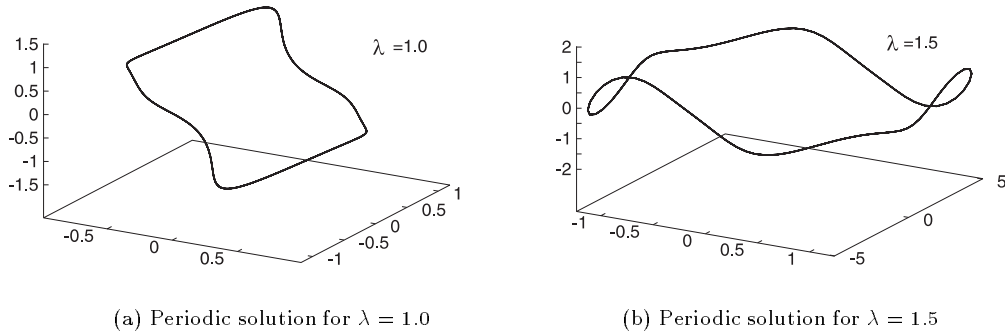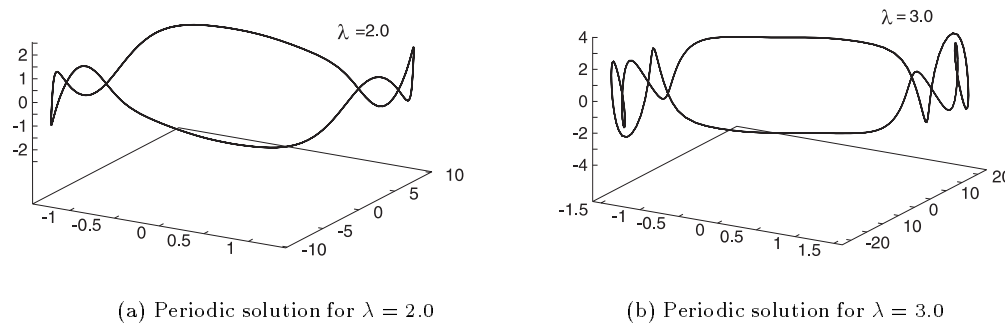

(a) Periodic solution for $\lambda = 1.0$ (b) Periodic solution for $\lambda = 1.5$

Fig. 4: Periodic solutions in coordinates (x_S, y_S, z_S)

(a) Periodic solution for $\lambda = 2.0$ (b) Periodic solution for $\lambda = 3.0$

Fig. 5: Periodic solutions in coordinates (x_S, y_S, z_S)

(a) Periodic solution for $\lambda = 1.0$ (b) Periodic solution for $\lambda = 1.5$
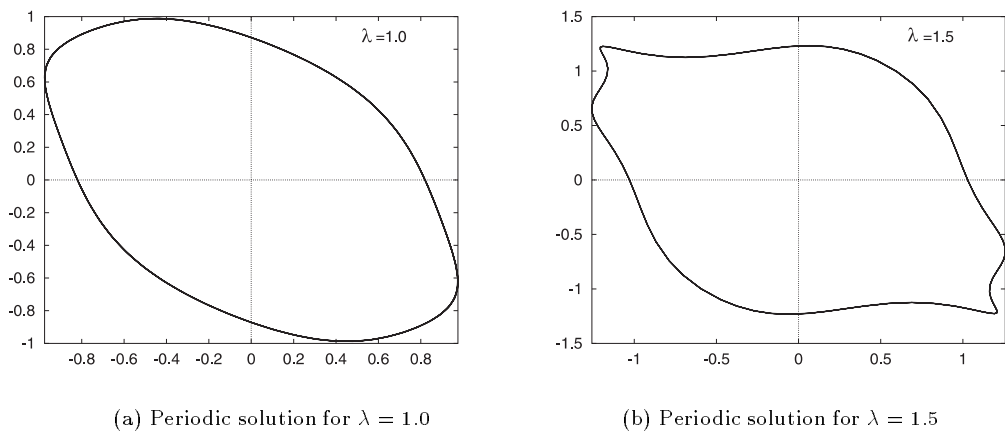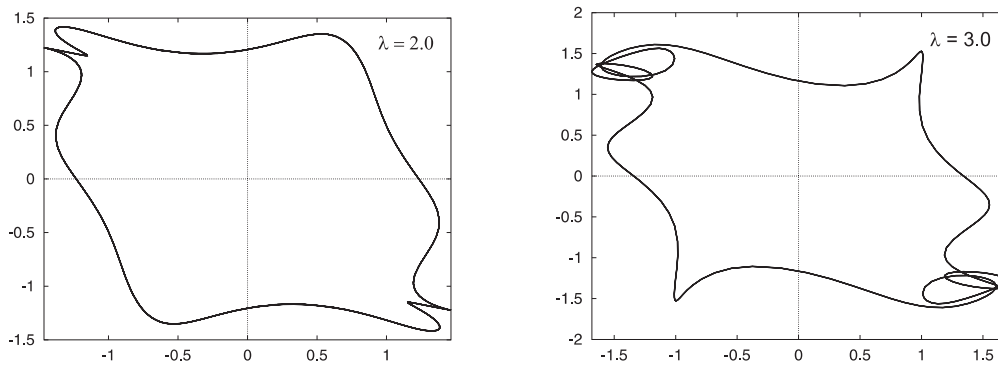
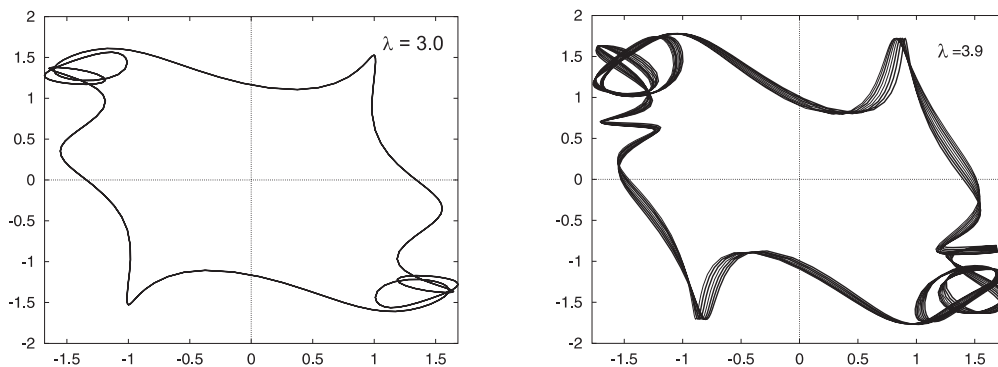**Fig.** 6: Periodic solutions in coordinates (x_R, x_S)

(a) Periodic solution for $\lambda = 2.0$ (b) Periodic solution for $\lambda = 3.0$

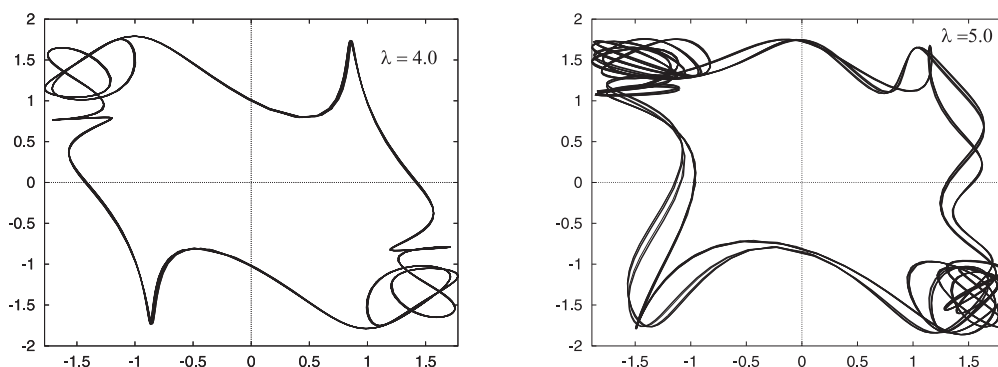**Fig.** 7: Periodic solutions in coordinates (x_R, x_S)

- At $\lambda \approx 3.2681$ an unstable solution arc bifurcates from this stable solution by a *fold (D-type) bifurcation*. For greater values of λ , further bifurcations arise.

- For $\lambda \approx 3.85$ the unstable solution has a complex pair of Floquét multipliers (quasi-periodic solution), which crosses the unit circle at $\lambda = 3.940668988$ by a *Hopf (H-type) bifurcation* (see Figs.8, 9 and Tab. 1).

(a) Periodic solution for $\lambda = 3.0$ (b) Quasi-periodic solution for $\lambda = 3.9$

Fig. 8: Periodic and quasi-periodic solutions in coordinates (x_R, x_S)

(a) Periodic solution for $\lambda = 4.0$ (b) Period-doubled solution for $\lambda = 5.0$

Fig. 9: Periodic and period-doubled solutions in coordinates (x_R, x_S)

- Finally at $\lambda = 5.3$ a *chaotic solution* of this model could be detected, which behaves like a bi-stable system (see Fig.10).

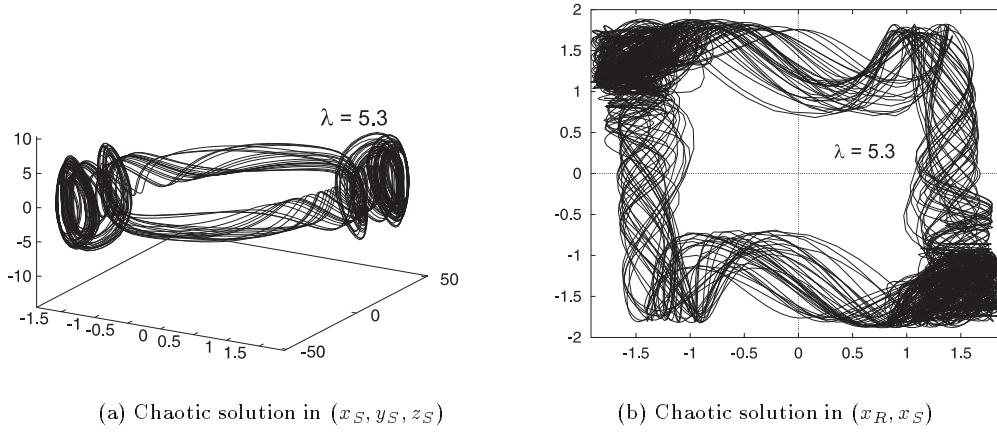- Behind this chaotic region at $\lambda = 6.0$ the system hasa *stable periodic* response (see Fig.11).

(a) Chaotic solution in (x_S, y_S, z_S)

(b) Chaotic solution in (x_R, x_S)

Fig. 10: Chaotic Solution for $\lambda = 5.3$

(a) Chaotic solution for $\lambda = 5.2$
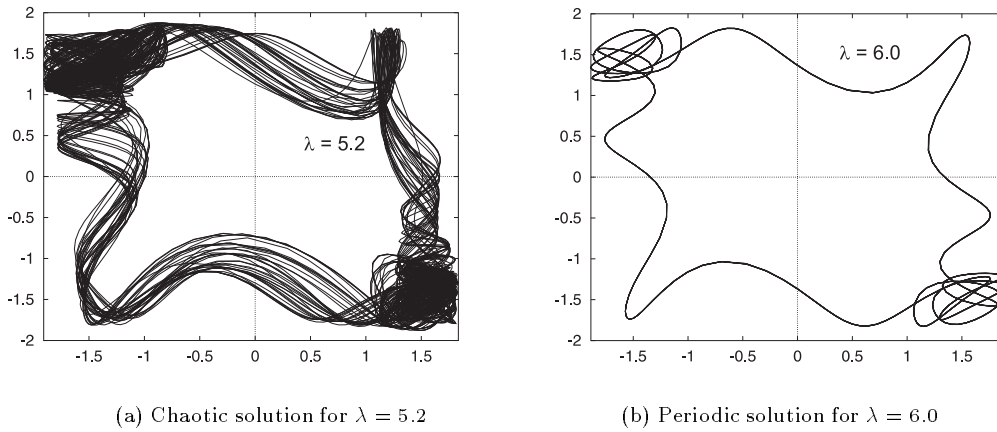
(b) Periodic solution for $\lambda = 6.0$

Fig. 11: Chaotic and periodic solutions in coordinates (x_R, x_S)

4 Approximation of Stable and Unstable Manifolds

For hyperbolic fixed points x^* of the Poincaré map (stroboscopic map) P the Stable Manifold Theorem guarantees the existence of *stable and unstable manifolds* $W^s(x^*)$, $W^u(x^*)$ tangential to the eigenspaces E^s and E^u. These manifolds can be approximated numerically in the case of the 2nd order model without coupling

$$\frac{d^2 x}{d\tau^2} + \delta \frac{dx}{d\tau} + \alpha x + \gamma x^n = -\hat{\Gamma} \cos \tau \tag{17}$$

by a geometrical algorithm described in [3].

Application of the continuation method
to this model equation with parameters $n = 9$; $\delta = 0.15$; $\alpha = 0.65$; $\gamma = 0.75$; $T = 4\pi$ yields the following results:

Tab. 1: Continuation of a Periodic Solution

λ	Floquét multipliers m_1, m_2, m_3	Spectral radius $\varrho = \max|m_i|$	Type of solution
1.0	6.3875E-1 6.2968E-1 7.1041E-3 +2.0812E-2*j	6.38756E-1	stable
2.0	2.1611E-1 -1.4926E-2 +4.2658E-2*j -1.4926E-2 -4.2658E-2*j	2.16116E-1	stable
3.0	3.8294E-1 9.5958E-2 -3.6799E-3 +3.3982E-2*j	3.82949E-1	stable
3.273	1.0049E+0 -4.6643E-2 -8.4952E-2*j -4.6643E-2 +8.4952E-2*j	**1.00499E+0**	**Fold-** (D-type-) bifurcation
3.8	1.1111E+0 9.8612E-1 -1.4840E-2 +1.5307E-2*j	1.11113E+0	*unstable*
3.85	1.0418E+0 +2.8871E-2*j 1.0418E+0 -2.8871E-2*j -1.4142E-2 +1.6228E-2*j	1.04221E+0	*unstable*
3.9	1.0224E+0 +7.0124E-2*j 1.0224E+0 -7.0124E-2*j -1.3486E-2 +1.7161E-2*j	1.02483E+0	*unstable*
3.940	9.9658E-1 +8.9890E-2*j 9.9658E-1 -8.9890E-2*j -1.3031E-2 +1.7992E-2*j	**1.00063E+0**	**Hopf-** (H-type-) bifurcation
4.0	9.3596E-1 -1.0938E-1*j 9.3596E-1 +1.0938E-1*j -1.2305E-2 +1.9455E-2*j	9.42334E-1	stable
4.3	1.1604E-1 +1.0951E-2*j 1.1604E-1 -1.0951E-2*j 7.2586E-2 +2.5850E-2*j	1.16565E-1	stable

Code: TABHET, Period: $T = 2\pi$, Precision: $tol = 10^{-10}$

- For $\hat{\Gamma} = 2.08$ the fixed point $P_2 = (-1.32525; -0.73182)$ of saddle type has non-intersecting invariant manifolds (see Fig.12(a)), whereas the fixed points P_{21} and P_{22} are stable. By increasing the amplitude $\hat{\Gamma}$ a *period doubling* occurs. For $\hat{\Gamma} = 2.15$ the fixed points P_{21} and P_{22} are of saddle type.
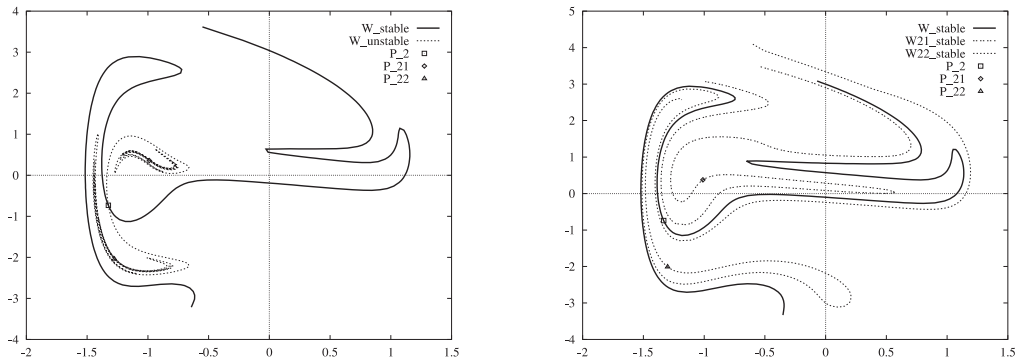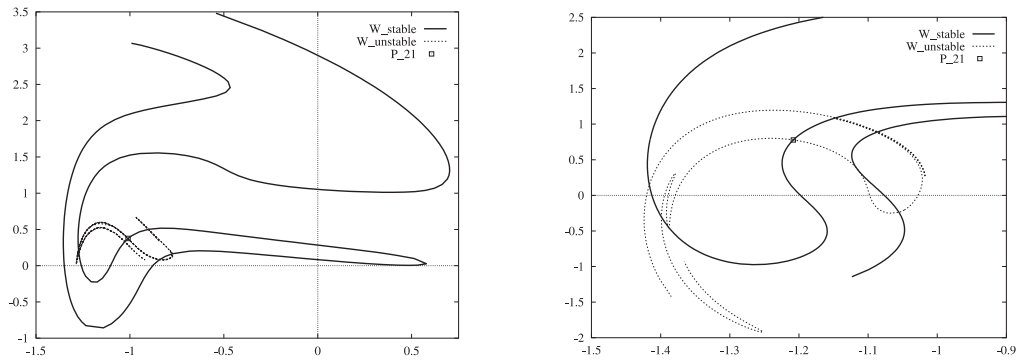
(a) Manifolds of P_2 for $\hat{\Gamma} = 2.08$ (b) Manifolds for $\hat{\Gamma} = 2.15$

Fig. 12: Invariant manifolds and fixed points

- After continuation of the 3 fixed points up to $\hat{\Gamma} = 2.15$ we now approximate (see Fig.12(b)) their stable manifolds $W^s(P_2)$, $W^s(P_{21})$, $W^s(P_{22})$. The curve $W^s(P_2)$ as a *separatrix* divides the regions of the other invariant manifolds.

- In Fig.13(a) we restrict the method to the fixed point $P_{21} = (-1.01019; 0.37511)$. Here the invariant curves $W^s(P_{21})$ and $W^u(P_{21})$ *intersect transversally* at homoclinic points $P_H \neq P_{21}$. Due to the **Smale-Birkhoff Theorem** (see [5]) the Poincaré-map has an imbedded horseshoe-like map as an indicator of chaos.

(a) Manifolds of P_{21}, $\hat{\Gamma} = 2.15$ (b) Manifolds of P_{21} for $\hat{\Gamma} = 3.0$

Fig. 13: Intersection of invariant manifolds

- This observation also holds for greater values of the amplitude $\hat{\Gamma}$. Fig. 13(b) shows a zooming for $\hat{\Gamma} = 3.0$ in the neighbourhood of the fixed point P_{21} where transversal homoclinic points are displayed.

5   Conclusion

This general model seems to be well-suited for describing energetic systems with nonlinear behaviour. As a first step ist is advisable to analyse numerically special models and to use their results as an information for the treatment of the general model.

References

[1] E. Philippw, <u>Der ferromagnetische Spannungsstabilisator</u>. Akademische Verlagsgesellschaft Geest & Portig K.-G., Leipzig 1968

[2] E.S. Philippow, W.G. Büntig, <u>Analyse nichtlinearer dynamischer Systeme der Elektrotechnik</u>. München, Wien: Carl Hanser Verlag, 1992

[3] W.G. Büntig, W. Vogt, <u>Non-Linear Basic Circuits for Modelling Energetic Systems</u>. Proceedings International Symposium on Non-Linear Electromagnetic Systems, Braunschweig 1997

[4] K. Bernet, W. Vogt, "Anwendung finiter Differenzenverfahren zur direkten Bestimmung invarianter Tori", Z. Angew. Mathematik u. Mech. Vol. 74, 1994, T577 - T579

[5] Y.A. Kuznetsov, <u>Elements of Applied Bifurcation Theory</u>. New York, Berlin, Heidelberg: Springer-Verlag, 1995

Authors:

Dr.-Ing. W.G. Büntig and Priv.Doz.Dr. W. Vogt
Technical University of Ilmenau
Dept. Fundamentals and Theory of Electrical Engineering and Dept. of Mathematics
D-98684 Ilmenau GERMANY
Tel.: +49-03677- 69 11 53, Fax: +49-03677-69 11 52, E-mail:buentig@e-technik.tu-ilmenau.de
Tel.: +49-03677- 69 32 66, Fax: +49-03677-69 32 70, E-mail:vogt@mathematik.tu-ilmenau.de